Solution structure of the DNA binding domain of a nucleoid-associated protein, H-NS, from *Escherichia coli*

Heisaburo Shindo[a,*], Takanobu Iwaki[a], Ryoichi Ieda[a], Hitoshi Kurumizaka[a], Chiharu Ueguchi[b], Takeshi Mizuno[b], Soichi Morikawa[c], Haruki Nakamura[c], Hitoshi Kuboniwa[d]

[a]*Tokyo University of Pharmacy and Life Science, Horinouchi, Hachioji, Tokyo 192-03, Japan*
[b]*School of Agriculture, Nagoya University, Chikusa-ku, Nagoya 464, Japan*
[c]*Protein Engineering Research Institute, Furuedai, Suita 565, Japan*
[d]*Chugai Pharmaceutical Inc., Gotenba, Shizuoka 412, Japan*

Received 27 December 1994; revised version received 13 January 1995

Abstract The three-dimensional structure of the C-terminal domain (47 residues) obtained from the hydrolysis of H-NS protein with bovine trypsin was determined by NMR measurements and distance geometry calculations. It is composed of an antiparallel β-sheet, an α-helix and a 3_{10}-helix which form a hydrophobic core, stabilizing the whole structure. This domain has been found to bind to DNA. Possible DNA binding sites are discussed on the basis of the solution structure of the C-terminal domain of H-NS.

Key words: H-NS; NMR; Solution structure; DNA binding protein

1. Introduction

H-NS (also called H1) was first identified as a major component of the *E. coli* nucleoid [1–3], which has been implicated in the condensation of the chromosome and in organization of prokaryotic nucleoid structure. It has no sequence homology to other well-characterized nucleoid-associated proteins such as HU and IHF (for review, see [4]). Recent extensive studies on the biological functions demonstrated that H-NS plays a role in the regulation of many apparently unlinked genes on the *E. coli* chromosome, and represses generally the expression of a variety of proteins at the level of transcription, either by binding directly to DNA or through changes in DNA topology [5–10].

H-NS protein contains many charged amino acids, but is a neutral protein composed of 137 amino acids [11]. It exists in solution predominantly as a homodimer [12]. Although H-NS is characterized as a relatively non-specific DNA-binding protein, its noticeable feature among other nucleoid proteins is to exhibit a preference for curved DNA sequences [7,13–14]. Thus, the transcriptional inhibition by H-NS is thought to result from its binding to the promoters which often contain curved DNA sequences [7,8,15]. In spite of such interesting DNA binding properties of H-NS, no structural information is available to date. To address this issue, we therefore attempted to investigate the structure of H-NS by NMR spectroscopy.

In this study, as the first step, a C-terminal fragment of H-NS extending from A91 to Q137 was isolated by means of trypsin-digestion, that retains a DNA-binding ability if not completely. The three-dimensional structure of this fragment was determined by two-dimensional proton NMR spectroscopy, and the results were discussed with emphasis on its biological function.

2. Materials and methods

2.1. Materials

H-NS protein was isolated from *E. coli* strain BL21 with plasmid pHOP11 [16] carrying an overexpression systems for the H-NS gene, and purified by precipitation with ammonium sulfate (40–60%), passed through phosphocellulose column, followed by heparin Sepharose column chromatography (Pharmacia). For NMR measurements the protein was extensively dialyzed against a buffer containing 300 mM NaCl, 10 mM KH_2PO_4, pH 5.5, and concentrated by centrifugation with Centriprep-10 (Amicon).

Purified H-NS protein was digested with bovine trypsin (Sigma) at a molar ratio of 1:5000 to protein in 0.5 M NaCl, 100 mM KP_i (pH 7.5) at room temperature for 1 h, and the reaction was terminated by an addition of phenylmethylene sulfonylfluoride (PMSF; Sigma) to a final concentration of 2. The reaction mixture was subjected onto heparin Sepharose column with a salt gradient of 0 to 0.8 M NaCl in 10 mM KP_i buffer, pH 7.5. The elutants were collected, heated at 90°C for 3 min to deactivate added trypsin, dialyzed against distilled water, and lyophylized. Meanwhile, the void fraction on the heparin column at 0 M NaCl was further applied onto DEAE Cellulofine A-500 column (Seikagaku Kogyo) in a salt gradient manner. All the purified fragments were subjected to the N-terminal amino acid sequence analysis. For NMR measurements the lyophylized sample was dissolved in 90% H_2O/10%D_2O or D_2O with 100 mM NaCl, 10 mM KH_2PO_4, pH 5.5 (direct meter reading).

Plasmid pMS101, a derivative of pUC19 containing a tandem sequence $d(GGCAAAAAC)_{12}$ cloned at the *Bam*HI site was digested with *Eco*RI and *Pst*I endonucleases (Takara), and the digestion fragment was isolated by soaking the appropriate pieces of the gel band on 12% polyacrylamide gel electrophoresis and purified by precipitation with ethanol. The sequence analysis showed that the fragment was 161-bp long with the tandem repeat mentioned above.

2.2. Electrophoresis

The *Eco*RI/*Pst*I fragment from plasmid pMS101 was labeled with [α-^{32}P]dATP (Amersham) using Klenow fragment (Takara). The end-labeled DNA was isolated by 12% polyacrylamide gel electrophoresis. The purified DNA pellet was dissolved and diluted with a binding buffer (10 mM Tris-HCl, pH 7.5, 80 mM NaCl, 1 mM EDTA, 10 mM 2-mercaptoethanol). A 0.3 pmol solution of the DNA and varying concentrations of H-NS or trypsin-digested fragments were mixed in 30 ml aliquots of the buffer solution and incubated at room temperature for 20 min, and then the binding mixtures were applied onto 8% non-denaturing polyacrylamide gel electrophoresis in 98 mM Tris-borate (pH 8.3), 2 mM EDTA at 4°C, 10 V/cm and autoradiographed.

2.3. NMR measurements

Two-dimensional proton NMR spectra were recorded at 27°C on a JEOL GX-500 spectrometer. Nuclear Overhauser effect spectroscopy (NOESY) experiments [17] were performed with mixing times of 100, 150 and 250 ms. Total correlation spectroscopy (TOCSY) experiments [18] were performed using a WALTZ-17 sequence [19] with mixing

*Corresponding author. Fax: (81) (426) 76-4542.

SSDI 0014-5793(95)00079-8

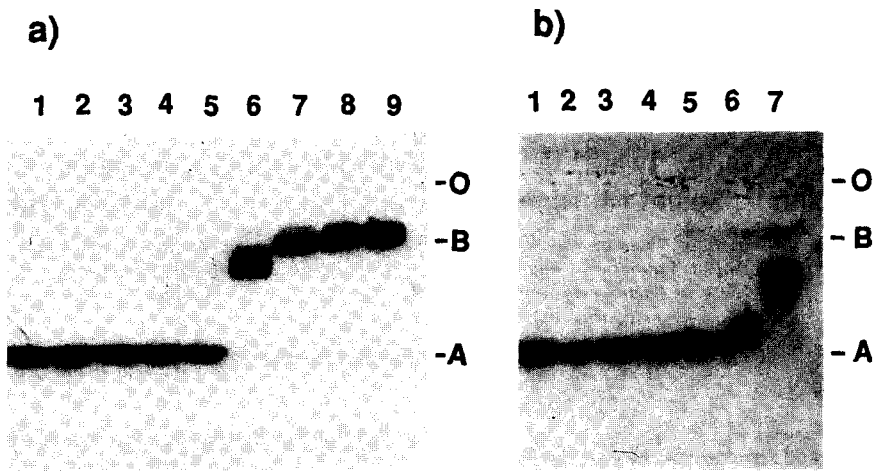

Fig. 1. Gel shift assay for the binding of H-NS and HNS48C to the curved DNA with a tandem repeat, d(GGCAAAAAAC)$_{12}$. The capital letters, A, B and O in the figure represent free-DNA, DNA-protein complex and the origin, respectively. The concentration of DNA in the binding buffer was 1.0×10^{-8} M. (a) For H-NS, the molar ratios of H-NS to DNA are: lane 1 = 0; lane 2 = 2; lane 3 = 4; lane 4 = 8; lane 5 = 16; lane 6 = 32; lane 7 = 64; lane 8 = 128; lane 9 = 256. (b) For HNS48C, the molar ratios of HNS48C to DNA are: lane 1 = 0; lane 2 = 4.1×10^3; lane 3 = 8.2×10^3; lane 4 = 16.4×10^3; lane 5 = 33×10^3; lane 6 = 65×10^3; lane 7 = 131×10^3.

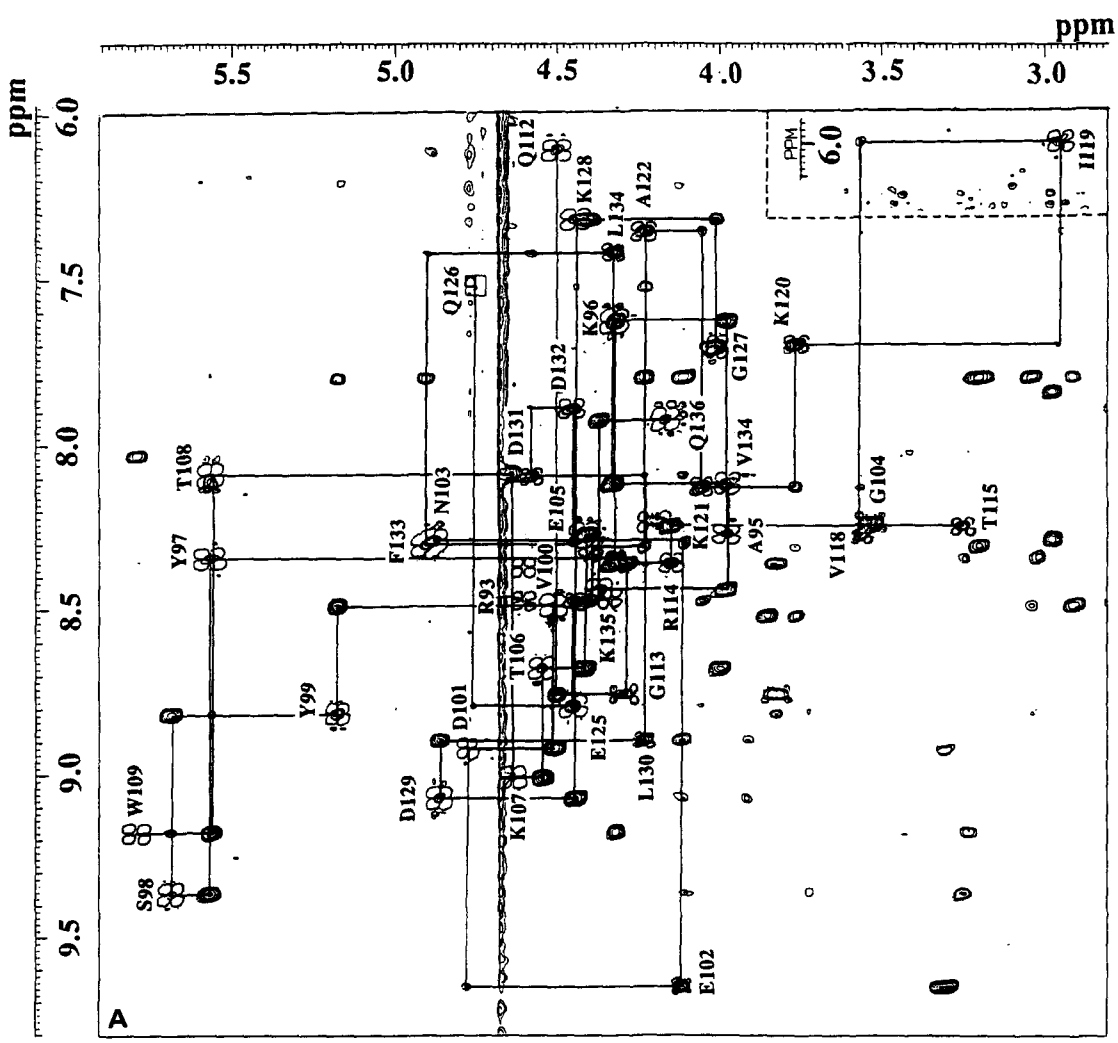

Fig. 2. Superpositions of the fingerprint regions of NOESY and DQF-COSY spectra of the C-terminal fragment, HNS47C (A), and intact H-NS (B) for comparison. Sequential assignments based on NOE and ^{3}J-coupling connectivities are drawn.

times of 55 and 105 ms. All the spectra mentioned above were acquired in 90% H_2O/10% D_2O or in D_2O under pre-saturation for solvent suppression, usually with 1K real t2 data points and 512 increments in t1 domain. Double-quantum filtered correlation spectroscopy (DQF-COSY) [20] was acquired with the same size as above and also with 2K real in t2 and 1K increments in t1 for estimating ^{3}J-coupling constants. J values were directly measured from the DQF-COSY spectrum.

Data matrices from NOESY and TOCSY experiments were processed with zero-filling in both t2 and t1 time domains and with multiplications of a Lorentz-Gaussian function (typically LB = −13 Hz and GB = 15 Hz in t2 and LB = −11 and GB = 18 Hz in t1) prior Fourier transformation. DQF-COSY data sets were processed with an unshifted sine bell applied in both t2 and t1 time domains.

2.4. Determination of the three-dimensional structure

The intensities of NOE cross peaks in the NOESY spectrum obtained with a mixing time of 150 ms were presented by peak height, and classified into strong, medium, weak and very weak NOEs. Each NOE intensity is converted into four upper distance limits depending upon two categories, NOEs between backbone protons and NOEs when side chain protons are involved, essentially according to the method of Wüthrich [21]. Structure calculations were carried out using 4-dimensional-simulated annealing (4D-SA) protocol with the program EMBOSS [22] and the conformers with the lowest distance violations were subjected to the restrained energy minimization using the program PRESTO [23] with the AMBER all-atom force field [24]. The ensemble or mean structure of the resulting conformers was used to represent the solution structure of the C-terminal domains in H-NS protein.

3. Results and discussion

3.1. Isolation of trypsin-digested fragments of H-NS

The hydrolysis of H-NS with bovine trypsin yielded fragments with certain sizes. The digests at 60 min were subjected to a preparative chromatography with heparin-Sepharose. In addition to a void fraction, two main peaks were eluted at about 0.4 M and 0.6 M NaCl in a NaCl salt gradient on the chromatography. Proteins in the void fraction were further separated on a DEAE column, and a polypeptide with an apparent molecular weight of 9000 was obtained at about 0.4 M NaCl, albeit with a very low yield. Its N-terminal amino acid sequence was determined to be SEALK, indicating that this particular fragment was derived from the N-terminal (thus, designated as HNS-N). On the other hand, the major elutant from the heparin-Sepharose column (at 0.2 M NaCl) was found to contain a highly homologous polypeptide, and its N-terminal amino acid sequence was determined to be AQRPAKY, indicating that this fragment contains a C-terminal portion of H-NS. Furthermore, an NMR spectral analysis (vide infra) of the fragment showed that it contains the C-terminal Q137 of intact H-NS, thereby extending from A91 to Q137. This C-terminal fragment containing 47 amino acids was termed HNS47C.

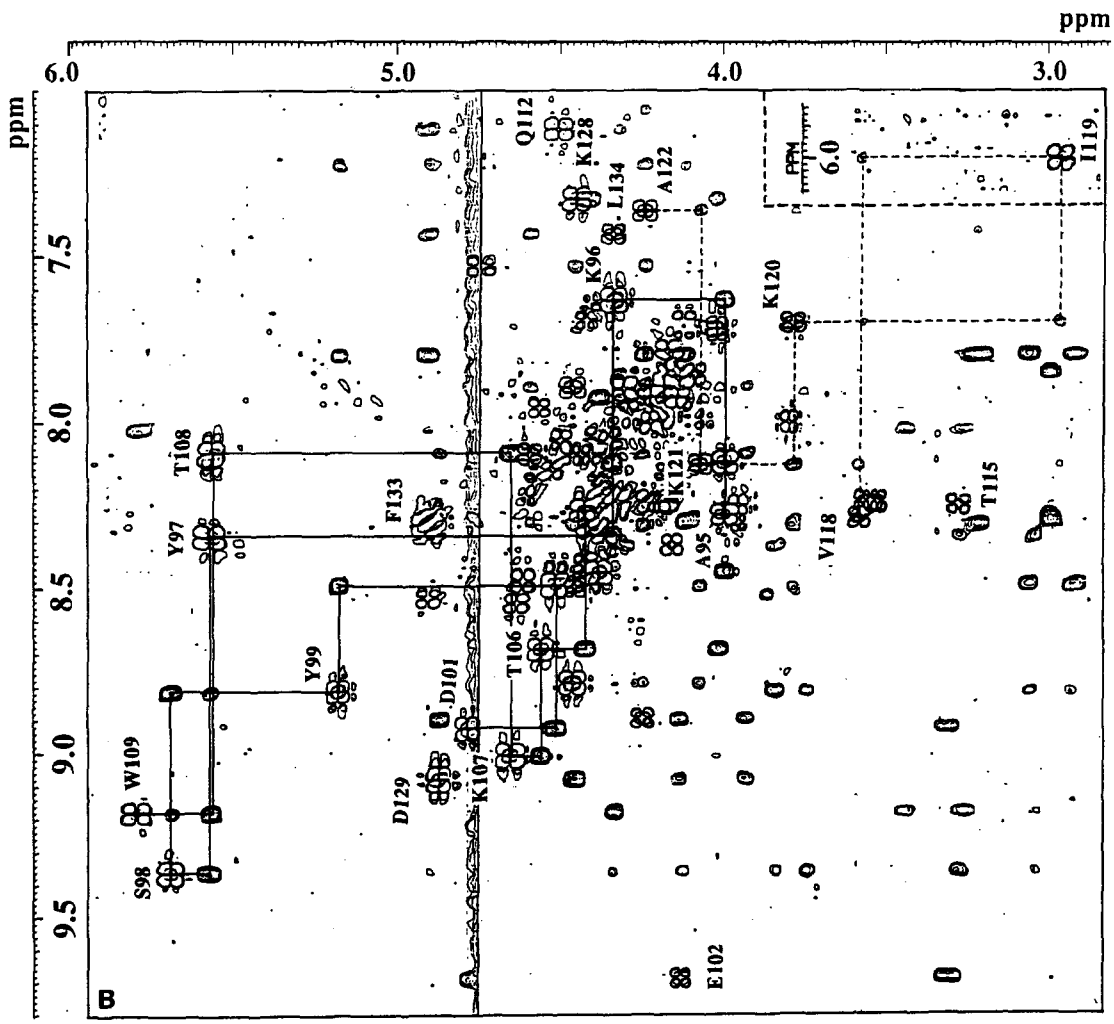

Fig. 2. (*Continued*).

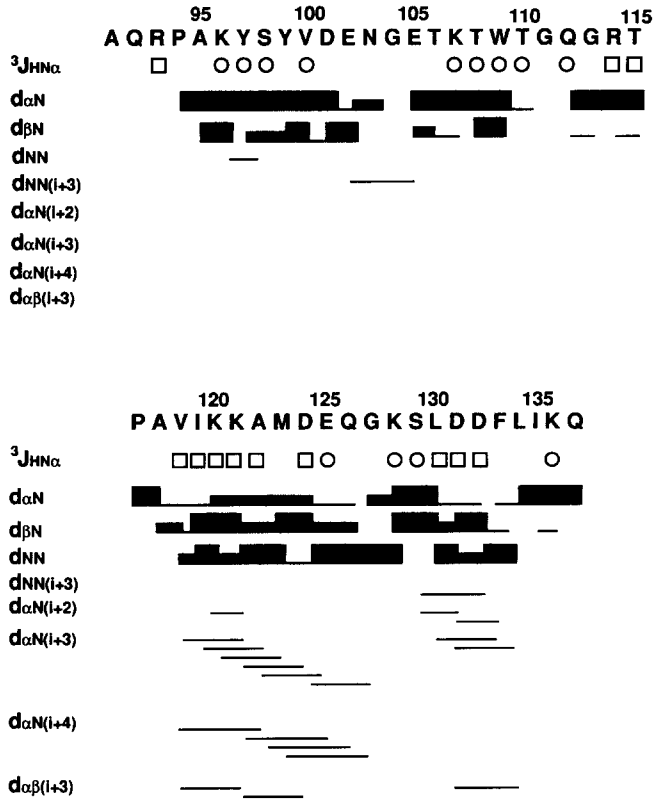

Fig. 3. Summary of sequential and medium ranges of NOE connectivities, $^3J_{HN\alpha}$ coupling constants for the backbone protons of HNS47C. NOE intensities are conventionally classified into strong, medium and weak (and very weak) as indicated by corresponding thickness of the bars. The values of $^3J_{HN\alpha}$ coupling constant less than 8 Hz are presented by the circles, and those equal or greater than 10 Hz are presented by the squares.

These two fragments, HNS-N and HNS47C, were analyzed in terms of their DNA-binding abilities by means of gel shift assay with ^{32}P-end labeled DNA fragment as a probe, which is 161-bp in nucleotides with a repetitive sequence of d(GGCAAAAAC)$_{12}$ at the center. This probe is known to represent the curved DNA sequence, as demonstrated previously [25]. Various amounts of intact H-NS, HNS-N, or HNS47C were incubated with the DNA probe in 10 mM phosphate buffer (pH 7.0) containing 50 mM NaCl, following by non-denaturing polyacylamide gel electrophoresis. The result is shown in Fig. 1, demonstrating that H-NS and HNS47C are able to bind to the DNA fragment, while HNS-N is not (data not shown). It should be noted, however, that the apparent dissociation constants, K_d, were estimated to be 2.5×10^{-7} and 1×10^{-3} M for intact H-NS and HNS47C, respectively, based on the quantitative analysis of the autoradiograms (Fig. 1). Although the binding affinity of HNS47C to DNA is much weaker by at least three orders of magnitude than that of H-NS, it is certainly capable of binding to DNA, suggesting that the DNA binding domain is located, at least in part, in the C-terminal region of H-NS.

3.2. Spectral assignments and secondary structure of HNS47C

HNS47C contains 4 aromatic residues (2 Tyr, 1 Phe and 1 Trp). The types of these ring protons were easily identified by their characteristic spin systems in DQF-COSY and TOCSY and NOESY spectra in D_2O as well as in H_2O. As for the tryptophan, $C^{\delta 1}$ and $N^{\delta 1}$ indole ring protons were identified from the characteristic singlet pattern and downfield-shifted peaks, and one out of remaining 4 ring protons, $C^{\zeta 2}$ proton, was identified by its NOE from neighboring $N^{\varepsilon 1}$ proton observed in H_2O. Finally remaining 3 ring protons in the tryptophan residue were assigned by the sequential spin-coupling connectivities from the $C^{\zeta 2}$ proton. The assignments for all the ring protons were confirmed by TOCSY. The C^{α} protons of the above aromatic residues were assigned based on NOEs between C^{α} or C^{β} protons and C^{δ} ring protons in each residue, which were used as markers for sequential assignments of C^{α} and amide protons as shown in Fig. 2A.

Fig. 2A shows the sequential connectivities in the fingerprint regions of the superimposed spectra of DQF-COSY and NOESY observed for HNS47C and Fig. 2B shows those of intact H-NS for comparison. In Fig. 2A, NOE connectivities

Table 1
Numbers of parameters and the results of distance geometry calculations for the C-terminal domain of H-NS

Structural parameters	Number of parameters	SA_i (rmsd)[a]	$<SA>_{ref}$[b]
RMS distance deviations (Å)			
Total	257	0.0187 (0.0009)	0.0167
intraresidue	65		
interresidue sequential ($\|i-j\| = 1$)	100		
interresidue short range ($1 < \|i-j\| \geq 5$)	26		
interresidue long range ($\|i-j\| > 5$)	66		
Deviations from idealized geometry			
bonds (Å)	751	0.005 (0.0002)	0.004
angles (degree)	1361	0.603 (0.020)	0.542
impropers (degree)	122	0.319 (0.033)	0.308
omega (degree)	44	7.507 (0.96)	6.32
Energetic statistics (kcal/mol)			
E_{dist}		3.13 (0.41)	2.46
$E_{L\ J}$		−181.8 (8.4)	−179.8
E_{total}		−245.2	−339.0

[a]The average values for the variables obtained from the final 16 refined structures. Numbers in parentheses are the standard deviations.
[b]$<SA>_{ref}$ represents the average structure of the final 16 structures. They were least square fitted each other using the coordinates of residues from Tyr97 to Glu101, from Thr106 to Trp109, from Ala117 to Glu125 and from Leu130 to Phe133, because of the disordered structures of the loops (see the text).

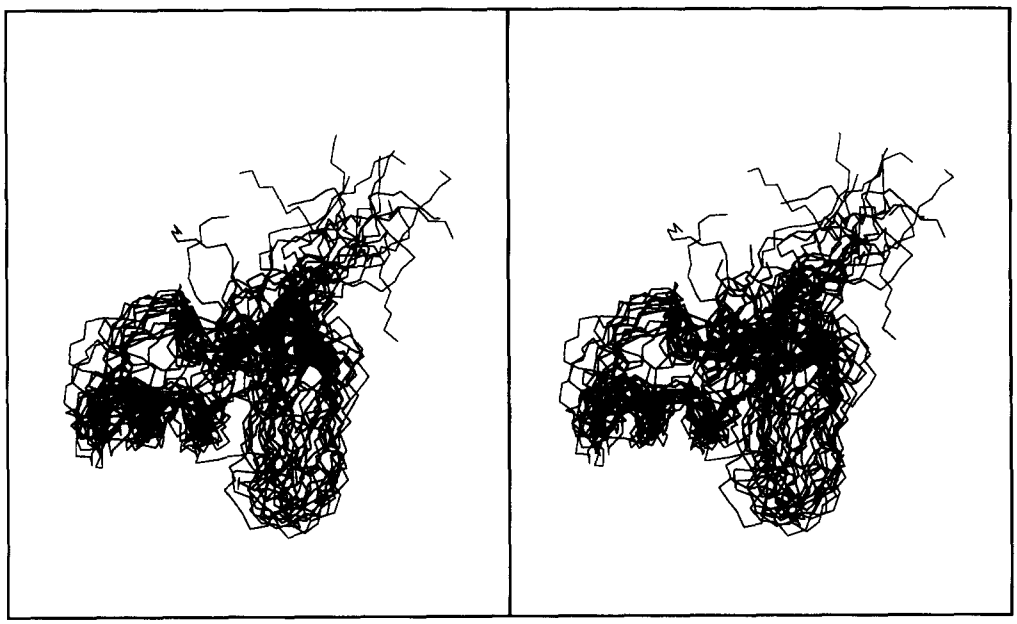

Fig. 4. Stereoview of superimposed backbone traces of 16 energy-minimized best structures of HNS47C.

between $C^{\alpha}H_{(i)}$ and $NH_{(i+1)}$, or $C^{\alpha}H_{(i)}$ and $C^{\delta}H_{(i+1)}$ for prorine were completed from residues P94 to W109, Q111 to T115, P116 to Q126 and G127 to Q137 (C-terminal end of H-NS).

Two notable features should be mentioned. The amide, C^{α} protons and C^{γ} methyl protons of I119 were abnormally upfield-shifted, probably due to a strong ring current effect, and two residues A91 in the N-terminus and G111 could not be identified, probably due to high flexibility of these regions.

In the spectra of intact H-NS as shown in Fig. 2B, most of backbone segments in the C-terminal domain of H-NS could be identified by very close similarity of the patterns in the sequential NOE connectivities found for HNS47C (Fig. 2A), indicating that HNS47C reserves the structure of the C-terminal domain in H-NS. However, most of C^{α}H-NH COSY corss peaks for the backbone protons in the N-terminal half of H-NS seems missing, the reason for which is not known at present.

The sequential and medium ranges of NOE connectivities were summarized in Fig. 3. In Fig. 3, an antiparallel β-sheet with a turn for segment K96-W109 is evident from strong NOEs for $d_{\alpha N}$ and $d_{\beta N}$, which was also evident from a strong NOE between C_{α} protons of S98 and T108 (data not shown). An α-helix structure for segment V118–G127 is also clear from strong or medium NOEs for d_{NN}, and weak NOEs for $d_{\alpha N(i+3)}$ or $d_{\alpha N(i+4)}$. A short 3_{10}-helix is suggested for segment L130–L134 from strong NOEs for d_{NN}, weak NOEs for $d_{\alpha N(i+3)}$ and $d_{\alpha N(i+2)}$, and no NOE for $d_{\alpha H(i+4)}$. These two helices were consistent with relatively smaller $^{3}J_{HN\alpha}$ coupling constants (<8 Hz) (see Fig. 3).

3.3. Three-dimensional structure of HNS47C

As listed in Table 1, a total of 257 NOEs comprising 65 intraresidual NOEs, 100 sequential ($|i-j| = 1$), 26 interresidual medium ($2<|i-j|\leq 5$) and 66 long range ($|i-j|>5$) NOEs were collected. The NOEs observed for amide protons were relatively small in number (ca. 5 NOEs per residue), indicating a fairly mobile structure of HNS47C. Based on these NOEs, the three-dimensional structure was calculated using 4D-SA with the program, EMBOSS [22]. Seventy-two structures with minimum distance violations were selected out of 200 calculated structures. Then, the conformation energy was minimized under above distance restrains using the program, PRESTO [23] with the AMBER all-atom force field [24]. Fig. 4 shows a superposition of the backbone heavy atoms of 16 refined structures. The overall atomic root-mean-square deviation (RMSDs) between the individual structures and the mean coordinate positions are 1.52 ± 0.29 Å for the backbone atoms and 2.22 ± 0.39 Å for all the heavy atoms, respectively. For the RMSD calculations, we used the coordinates of the well defined parts of the structure, including the antiparallel β-sheet, (Y97-

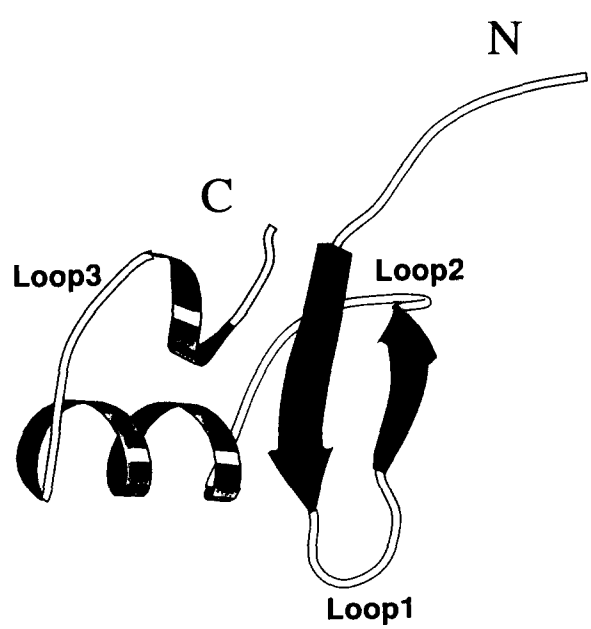

Fig. 5. A ribbon representation of the refined mean structure of HNS47C.

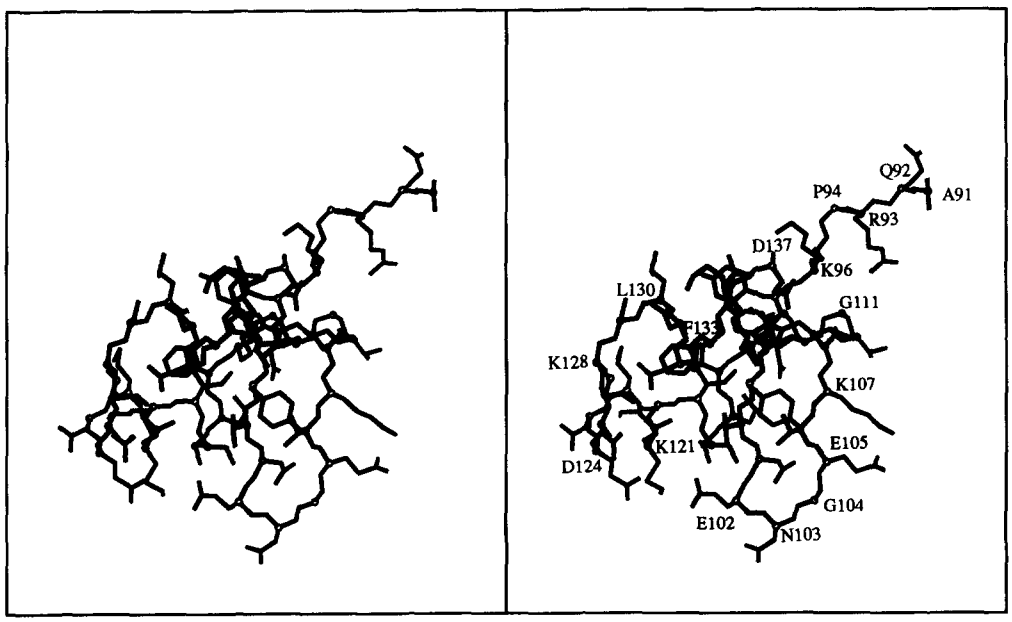

Fig. 6. Stereoview of a stick representation of all heavy atoms in the refined mean structure of HNS47C.

T101) and T106-W109, α-helix (A117–E125) and short 3_{10}-helix (L130–F133). Fig. 5 shows the ribbon drawing of the refined mean structure. The α-helix is located at the back side of the β-sheet and approximately perpendicular to it, while the 3_{10}-helix is at the side of the β-sheet. Loops 1, 2 and 3 between these secondary structures as well as the N- and C-termini are not well defined as shown in Fig. 4, probably because of high flexibility in these regions. Other statistics of the converged structures are sound as indicated in Table 1.

Among nucleoid-associated proteins HU is only the one whose structure is known [26]. HU dimer has a pair of protruding long β-sheets which are supposed to bind to the major groove of DNA. It is clear from the folded structure of HNS47C that H-NS has no structural homology to HU. We have surveyed DNA binding proteins or their DNA binding domains reported so far, but no homologous folds were found.

To see the solution structure in more detail the stereoview of the mean structure is shown in Fig. 6. A few points should be mentioned. First, a hydrophobic core composed of the side chains of 4 aromatic and two aliphatic residues (Y97, Y99, W109, F133, V118 and I119) is formed, which is a key stabilizing element for the folded structure of HNS47C. Second, the indole ring of W109 is right on the top of residue I119, which explains the abnormal upfield-shifts for C^{α}, NH and C^{γ} methyl protons of this residue owing to the ring current effect by the indole ring.

3.4. DNA binding sites of H-NS

The result of trypsin-digestion experiment suggested that there are at least two distinct structural domains in H-NS: one is an N-terminal domain with about 80 amino acids and the other is a C-terminal domain with 47 amino acids. It was found that the C-terminal fragment, whose structure was determined in this study, was capable of binding to DNA, although its affinity to DNA is much weaker as compared with that of intact H-NS. This may be explained by assuming that some other portions may be coordinately required for H-NS to fully contact with DNA, or alternatively by assuming that some other structural states (e.g. dimerization) may be essentially involved in the tight DNA-recognition. In any case, it is worth examining the structure of HNS47 with regard to its possible mode of DNA-recognition.

A variety of H-NS mutants with a certain amino acid substitution have been isolated and characterized (Ueguchi and Mizuno, unpublished results). Each mutant exhibits a remarkable phenotypic alteration, particularly with regard to the proU operon whose expression is known to be repressed directly by the H-NS binding to the promoter [9]. A number of such mutants were revealed to have a single amino acid alteration within the region corresponding to HNS47C. In this context, it is worth mentioning that the positions of altered amino acids appeared to be located non-randomly and clustered at certain locations, particularly at positions 90–95 and positions 110–115. These are within the loop-regions, the N-terminal and loop 2, of HNS47C (see Fig. 5 or 6), where the former region may form a loop since the region is accessible to the protease. These preliminary results support the idea that HNS47C represent an important domain in terms of the H-NS function including DNA-binding. Interestingly, no such mutant has been found in the regions of β-sheet and α-helix. This observation suggests that two loop regions instead of the rigid secondary structures may be directly involved in the DNA-binding.

In conclusion, H-NS may present a new DNA binding motif. Yet, any conclusive features on the DNA binding mode must wait until more detailed structural information of the H-NS-DNA complexes is available, including the role of the N-terminal domain.

Acknowledgements This work was supported by a grant-in-aid for Scientific Research from the Ministry of Education, Science and Culture of Japan (04254105). We express a great appreciation to Drs. T. Tanaka and T. Yamazaki of University of Toronto for helpful suggestions for the spectral assignments. We also thank Mrs. C. Sakuma of Tokyo University of Pharmacy and Life Science for her assistance for NMR measurements.

References

[1] Jacquet, M., Cukier-Kahn, R., Pla, J. and Gros, F. (1971) Biochem. Biophys. Res. Commun. 45, 1597–1607.
[2] Cukier-Kahn, R., Jacquet, M. and Gros, F. (1972) Proc. Natl. Acad. Sci. USA 69, 3643–3647.
[3] Varshavsky, A.J., Nedospasov, S.A., Bakayev, V.V., Bakayeva, T.G. and Georgiev, G.P. (1977) Nucleic Acids Res. 4, 2725–2745.
[4] Drilica, K. and Rouviere-Yaniv, J. (1987) Microbiol. Rev. 51, 301–319.
[5] Hulton, C.S.J., Seirafi, A., Hinton, J.C.D., Sidebothan, J.M., Waddell, L., Pavitt, G.D., Owen-Hughes, T., Spassky, A., Buc, H. and Higgins, C.F. (1990) Cell 63, 631–642.
[6] Göransson, M., Sondén, B., Nilsson, P., Dagberg, B., Forsman, K., Emanuelson, K. and Uhlin, B.E. (1990) Nature 344, 682–685.
[7] Owen-Hughes, T.A., Pavitt, G.D., Santos, D.S., Sidebothan, J.M., Hultpn, C.S.J., Hinton, J.C.D. and Higgins, C.F. (1992) Cell 71, 255–265.
[8] Ueguchi, C., Kakeda, M. and Mizuno, T. (1993) Mol. Gen. Genet. 236, 171–178.
[9] Ueguchi, C. and Mizuno, T. (1993) EMBO J. 12, 1039–1046.
[10] Lucht, J.M., Dersch, P., Kempf, B. and Bremer, E. (1994) J. Biol. Chem. 269, 6578–6586.
[11] Pon, C.L., Calogero, R.A. and Gualerzi, C.O. (1988) Mol. Gen. Genet. 212, 199–202.
[12] Falconi, M., Gualteri, M.T., La Teana, A., Losso, M.A., Pon, C.L. (1988) Mol. Microbiol. 2, 323–329.
[13] Yamada, H., Muramatsu, S. and Mizuno, T. (1990) J. Biochem. 108, 420–425.
[14] Bracco, L., Kotlarz, D., Kolb, A., Dielmann, S. and Buc, H. (1989) EMBO J. 8, 4289–4296.
[15] Yoshida, T., Ueguchi, C., Yamada, H. and Mizuno, T. (1993) Mol. Gen. Genet. 237, 113–122.
[16] Tanaka, K., Yamada, H., Yoshida, T. and Mizuno, T. (1991) Agric. Biol. Chem. 55, 3139–3141.
[17] Kumer, A., Ernst, R.R. and Wüthrich, K. (1980) Biochem. Biophys. Res. Commun. 95, 1–6.
[18] Davis, D.G. and Bax, A. (1985) J. Am. Chem. Soc. 107, 2820–2821.
[19] Bax, A., Sklemnar, V., Clore, G.M. and Gronenborn, A.M. (1987) J. Am. Chem. Soc. 109, 6511–6513.
[20] Rance, M., Sorensen, O.W., Bodenhausen, G., Wagner, G., Ernst, R.R. and Weuthrich, K. (1983) Biochem. Biophys. Res. Commun. 117, 479–485.
[21] Wüthrich, K. (1986) NMR of Proteins and Nucleic Acids, Wiley, New York, NY.
[22] Nakai, T., Kidera, A. and Nakamura, H. (1993) J. Biomolec. NMR 3, 19–40.
[23] Morikami, K., Nakai, T., Kidera, A., Saito, T. and Nakamura, H. (1992) Comput. Chem. 16, 243–248.
[24] Weiner, S.J., Kollman, P.A., Nguyen, D.T. and Case, D.A. (1986) J. Comput. Chem. 7, 230–250.
[25] Koo, H.S., Wu, H.M. and Crothers, D.M. (1986) Nature 320, 501–503.
[26] Tanaka, I., Krzysztof, A., Dijk, J., White, S.W. and Wilson, K.S. (1984) Nature 310, 376–381.